Reducing Computational Load in Moving-Horizon Observers using Partial explicit Map Inversion

Oumayma Omar and Mazen Alamir

Abstract— This paper proposes a novel approach that may help reducing the computational burden when using the Nonlinear Moving-Horizon Observer (MHO) technique. This technique is often used to reconstruct unmeasured quantities of a dynamic system. The latter may include both the state and the vector of parameters that are involved in the system model. The proposed approach is based on the use of partial explicit inversion maps that express a part of the problem unknowns as a function of the remaining one. The Moving-Horizon Observers can therefore concentrate on the latter reduced dimensional unknown vector. The paper shows how explicit inversion maps can be derived based on a recently developed graphical-signature-based technique. Two illustrative examples are proposed to show the efficiency of the proposed solution.

I. INTRODUCTION

It is needless to say that the problem of reconstructing unknown quantities from a limited set of measurement remains a key open problem in nonlinear systems theory. The reason is that the solution of the above problem underlines almost all classical dynamic systems paradigms such as measurement-feedback control, diagnosis, supervision and fault tolerant control to cite but a limited number of issues.

Algorithms that achieve this task are called observers. As far as nonlinear systems are concerned, many observation techniques have been developed during the last four decades. This includes high-gain observers [5], sliding-modes observers [12], Moving-Horizon Observers (MHO) [8] and naturally, the widely used Extended-Kalman-Filter (EKF) observer. Excellent reviews of nonlinear observer design techniques can be found in [11] and [4].

Amongst all possible observer design alternatives, MHO technique has witnessed an increasing interest these last years because of its ability to handle constraints and to fully exploit precise and generally nonlinear models of the dynamic processes under study. This observer requires on-line solution of a non convex optimization problem in which the cost function is the integral output prediction error while the decision variable is the set of unknown quantities to be recovered (state and unknown parameter vectors). The on-line solution of this optimization problem can be cumbersome to an extent that may questions the feasibility of the whole approach, at least for a family of

Authors are with Gipsa-lab, Control Systems Department, CNRS (French National Research Center). University of Grenoble `oumayma.omar(mazen.alamir)@grenoble-inp.fr/`

problems that needs high updating rates.

The aim of the present paper is to address this specific complexity reduction problem by using partial explicit map inversion. This is made possible when a part of the unknown vector can be made explicitly dependent on the remaining part. It is suggested that such a map inversion can be performed using graphical signature based classification tool that has been recently developed in a series of papers [13], [14], [15]. By doing so, the dimension of the decision variable to be updated on-line can be strongly reduced and the real-time implementability of the MHO algorithm is enhanced.

The paper is organized as follows: First, the key idea is clearly stated in section II where the central role played by the inversion map is underlined. Section III recalls the graphical signature-based classification framework and states the necessary conditions that are needed for it to be used in the inversion map derivation. The whole solution is then illustrated in section IV by two illustrative examples in order to make concrete the set of concepts invoked throughout the paper. Finally, section V concludes the paper and gives a road map for future investigations.

II. THE KEY IDEA

Let us consider a nonlinear system that admits the following general model:

$$x(k + i) = X(i, x(k), p, \mathbf{u}) \tag{1}$$

where $x \in \mathbb{R}^n$ is the state vector, $\mathbf{u}$ is the control profile that is applied during the time interval $[k\tau, (k + i)\tau]$ where τ is some sampling period. The vector $p \in \mathbb{R}^{n_p}$ gathers the model unknown parameters. Note that (1) may be obtained based on physical modeling involving Ordinary Differential Equations (ODEs), Partial Differential Equations (PDEs) or a more involved hybrid nonlinear model. It is assumed that measurements $y(k) := h(x(k), p) \in \mathbb{R}^{n_y}$ are periodically acquired and stored over some time window of length $T = N_O \cdot \tau$ to form the measurement data given by:

$$Y_m(k) := \begin{pmatrix} y(k - 1) \\ \vdots \\ y(k - N_O) \end{pmatrix} \in \mathbb{R}^{N_O \cdot n_y} \tag{2}$$

The use of Moving-Horizon Observer (MHO) for simultaneous state and parameter estimation is based on the

implicit assumption according to which there exists a map $\Psi : \mathbb{R}^{N_O \times n_y} \to \mathbb{R}^n \times \mathbb{R}^{n_p}$ such that:

$$(x(k), p) = \Psi(Y_m(k)) \qquad (3)$$

Otherwise, the simultaneous estimation problem would be theoretically infeasible. However, the existence of such a map does not mean that it can be explicitly available for observer design. That is the reason why MHO design relies on the implicit reconstruction of Ψ through the solution of the following optimization problem:

$$(\hat{x}(k - N_O), \hat{p}) :=$$
$$\arg\min_{(\xi, p)} \sum_{i=0}^{N_O - 1} \|y(k - N_O + i) - Y(i, \xi, p, \mathbf{u})\|^2 \quad (4)$$

leading to the state estimate given by

$$\hat{x}(k) = X(N_O, \hat{x}(k - N_O), \hat{p}, \mathbf{u})$$

Note that the optimization problem (4) has to be solved at each sampling period which may represent a challenging task in some cases. Despite this potential problem, softwares for MHO design are by now quite frequently proposed [3], [16], [1] with encouraging successful results. Nevertheless, it remains a fact that the MHO implementation can be made easier if the underlying optimization problem can be simplified by some off-line preliminary investigation. Such a scheme is proposed in the remainder of the present paper.

A. Partial Map Inversion

In order to simplify the notation, let us use $z := (\xi, p) \in \mathbb{R}^{n+n_p}$ to denote the decision variable in the optimization problem (4). Using this notation, the straightforward notation $X(i, z, \mathbf{u})$ and $Y(i, z, \mathbf{u})$ can be used to denote the trajectories of the state and the output starting from the initial conditions and the parameter vector value both contained in z, according to the original notation $X(i, (\xi, p), \mathbf{u})$ already used in (1). Moreover, the optimization problem (4) can be shortly rewritten as follows:

$$\hat{z} := \arg\min_z J\big(z \,|Y_m(k), \mathbf{u}\big) \qquad (5)$$

Now assume that the following assumption holds:

Assumption 1:
There exists a partition $z = \mathcal{Z}(z^{(1)}, z^{(2)})$ with $(z^{(1)}, z^{(2)}) \in \mathbb{R}^{n_1} \times \mathbb{R}^{n_2}$ such that for any given pair $(z^{(2)}, \mathbf{u})$, there exists an explicitly **invertible** map taking the following form:

$$T_{(z^{(2)}, \mathbf{u})} : \qquad \mathbb{R}^{n_1} \longrightarrow \mathbb{R}^{n_1} \qquad (6)$$
$$z^{(1)} \rightsquigarrow S\Big(\big\{Y(i, \mathcal{Z}(z^{(1)}, z^{(2)}), \mathbf{u})\big\}_{i=0}^{N_O - 1}\Big)$$

where S is a function that maps the sequence of measurements corresponding to the initial state and the vector of parameters defined by $(z^{(1)}, z^{(2)})$ and the control profile $\mathbf{u}$ into $\mathbb{R}^{n_1}$. $\qquad \odot$

More precisely, given $(z^{(2)}, \mathbf{u})$, for each $z^{(1)}$, the image of $T_{(z^{(2)}, \mathbf{u})}$ is constructed according to the following steps:

1) Compute $z = \mathcal{Z}(z^{(1)}, z^{(2)})$
2) Compute the output trajectory $\big\{Y(i, z, \mathbf{u})\big\}_{i=0}^{N_O - 1}$
3) Apply the map S

The key point in Assumption 1 lies in the invertibility of the map $T_{(z^{(2)}, \mathbf{u})}$ for any pair $(z^{(2)}, \mathbf{u})$ since this clearly leads to the following result:

Proposition 1:
If Assumption 1 holds, then, the $(n + n_p)$-dimensional optimization problem (5) can be solved by solving the $(n + n_p - n_1)$-dimensional problem given by:

$$\hat{z}^{(2)} := \arg\min_{z^{(2)}} J_r\big(z^{(2)} \,|Y_m(k), \mathbf{u}\big) \qquad (7)$$

where

$$J_r\big(z^{(2)} \,|Y_m(k), \mathbf{u}\big) :=$$
$$J\Big(\mathcal{Z}\big(T_{(z^{(2)}, \mathbf{u})}^{-1}(S(Y_m(k))), z^{(2)}\big) \,|Y_m(k), \mathbf{u}\Big) \quad (8)$$

where $T_{(z^{(2)}, \mathbf{u})}^{-1}$ is the inverse map that is supposed to be explicitly available by Assumption 1. Note that the term

$$T_{(z^{(2)}, \mathbf{u})}^{-1}(S(Y_m(k)))$$

is nothing but the expected value of $z^{(1)}$ if $z^{(2)}$ takes the true value that led to the measurement data $Y_m(k)$.

Section IV shows two examples with $n = 2$, $n_p = 1$ and $n_1 = 2$ meaning that an original 3-dimensional optimization problem can be replaced by a scalar optimization problem, after an appropriate inversion map is found off-line.

Needless to say that finding an explicitly invertible map like the one invoked in Assumption 1, is generally an extremely hard task. The main contribution of the present paper is to attract the reader attention to an approximate inversion technique that the authors found efficient on a variety of examples of which only two are shown here for the lack of space. The next section reminds the signature based classification tool that has been recently developed and successfully applied (see [13], [14], [15]).This tool is in the heart of the proposed approximate partial inversion map invoked in the above discussion since it is used to define the map S invoked in Assumption 1.

III. A GRAPHICAL SIGNATURE-BASED TOOL FOR MAP INVERSION

A. Definitions

Let $(z^{(2)}, \mathbf{u})$ be given; we consider the set $\mathbb{Z}^{(1)} \subset \mathbb{R}^{n_1}$ of admissible values of $z^{(1)}$ (say a hypercube of $\mathbb{R}^{n_1}$). Note that the map:

$$z^{(1)} \rightsquigarrow \big\{Y(i, \mathcal{Z}(z^{(1)}, z^{(2)}), \mathbf{u})\big\}_{i=0}^{N_O - 1} \qquad (9)$$

associates to each value $z^{(1)} \in \mathbb{Z}^{(1)}$ an output sequence of length N_O. Now let's take $N = N_O - M$ (for some integer M) and assume that there is a map $P : \mathbb{R}^{N+1} \to \mathbb{R}^2$ that associates to each output sequence $\mathcal{Y}$ of length $N + 1$, a

specific point $P(\mathcal{Y})$ in $\mathbb{R}^2$ (see Fig. 1). Applying this map to the M output sequences given by:

$$\left\{ \mathcal{Y}^{(i)}(z^{(1)}) := \begin{pmatrix} Y(N+i,\dots) \\ \vdots \\ Y(i,\dots) \end{pmatrix} \in \mathbb{R}^{N+1} \right\}_{i=0}^{M-1} \quad (10)$$

yields a $2D$ graphical signature (including M points) in the 2D plane. This signature is denoted hereafter as follows:

$$\mathcal{S}(z^{(1)}) := \left\{ \begin{pmatrix} \chi_i(z^{(1)}) \\ \eta_i(z^{(1)}) \end{pmatrix} := P(\mathcal{Y}^{(i)}(z^{(1)})) \in \mathbb{R}^2 \right\}_{i=0}^{M-1} \quad (11)$$

The function P that is needed to generate this signature is detailed in **Appendix A**.

To summarize, each measurement data contained in the observation window of length N_O can be represented by a 2D signature containing M points. As a matter of fact, the integer $N = N_O - M \geq 1$ is a free parameter that can be chosen to obtain different signatures (see Appendix A.), consequently, one may write $\mathcal{S}^{(N)}(z^{(1)})$ to explicitly express this fact.
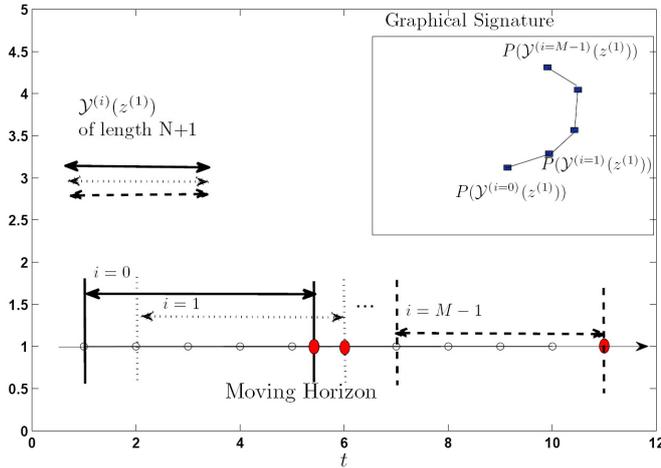

Fig. 1.   Signatures $\mathcal{S}^N$ obtained for successive output sequences $\mathcal{Y}^{(i)}(z^{(1)})$. For each one a point $P(\mathcal{Y}^{(i)}(z^{(1)}))$ in the 2D space $\mathbb{R}^2$ is associated.

B. Signature property

A map r that associates to each signature

$$\mathcal{S}^{(N)} := \left\{ \begin{pmatrix} \chi_i \\ \eta_i \end{pmatrix} \right\}_{i=0}^{M-1} \subset \mathbb{R}^2$$

a scalar[1] is called a *signature property*.

C. Measurement data coordinate

A pair $c = (\mathcal{S}^{(N)}, r)$ composed of a signature $\mathcal{S}^{(N)}$ and an associated property is called a measurement data coordinate (or shortly coordinate when no ambiguity holds).

[1]This may be $\max_i(\chi_i)$, $\max_i(\eta_i) - \min_i(\eta_i)$, $mean(\{\chi_i\}_{i=1}^N)$, $std(\{\eta_i\}_{i=0}^{M-1})$, $\max_i(\{\frac{\chi_i}{(\varepsilon + |\eta_i|)}\})$, $\dots$, etc.

D. Definition of the invertible map $T_{(z^{(2)},\mathbf{u})}(\cdot)$

For a given pair $(z^{(2)}, \mathbf{u})$, a typical definition of $T_{(z^{(2)},\mathbf{u})}(z^{(1)})$ invoked in Assumption 1 is given by:

$$T_{(z^{(2)},\mathbf{u})}(z^{(1)}) := \begin{pmatrix} r_1(\mathcal{S}^{N_1}(z^{(1)})) \\ \vdots \\ r_{n_1}(\mathcal{S}^{N_{n_1}}(z^{(1)})) \end{pmatrix} \quad (12)$$

where $c_i := (\mathcal{S}^{(N_i)}, r_i)$, $i = 1, \dots, n_1$ are n_1 conveniently chosen coordinates making (12) invertible over the admissible set $\mathbb{Z}^{(1)}$. The choice of these coordinates is done by visual inspection based on the investigation of different candidate values for N and r. The visual inspection is highly facilitated by the 2D character of the signatures. The examples proposed in the next section make easier the understanding of the proposed framework since concrete situations, signatures, properties and coordinates can be examined.

IV. Illustrative Examples

In section II we have clearly explained the inversion scheme that helps to reduce the complexity of optimisation problem invoked when using the MHO algorithm. In this section we will focus on the steps followed to find the invertible map (12); we will demonstrate how to find an appropriate graphical signature and how to choose a relevant system of coordinates. This one will help in finding a part of unknown variables depicted in (5) as off-line step of resolution.

A. Example 1

Let us first consider the reversible reaction [10]:

$$2A \xrightarrow{\bar{\beta}} B \quad (13)$$

with stoichiometric matrix $\upsilon = (-2, 1)$ and reaction rate $\bar{r} = \bar{\kappa}C_A^2$. The state and measurement vectors are respectively given by $x := (C_A, C_B)^T$ and $y = x_1 + x_2$. Assuming a perfect gas and a perfectly mixed isothermal reactor, the system equations write:

$$\dot{x} = f(x) = \upsilon^T \bar{r} = \begin{pmatrix} -2\bar{\beta}x_1^2 \\ \bar{\beta}x_1^2 \end{pmatrix} \quad (14)$$

$$y = x_1 + x_2 \quad (15)$$

which, in discrete time form leads to a system similar to (1) with two states x_1, x_2 and one parameter $\bar{\beta}$ that is assumed here to be unknown.

The framework proposed in section II is applied to this example using the following definitions:

- $z^{(1)} := (x_1, x_2)^T$, $n_1 = 2$, $z^{(2)} = \bar{\beta}$

- $\mathbb{Z}^{(1)} := [0,3] \times [0,3]$, $N_O = 11$, $\tau = 0.01$

Let us define the following discrete subset of $\mathbb{Z}^{(1)}$ that may be obtained using uniform grids on the admissible intervals for x_1 and x_2, namely:

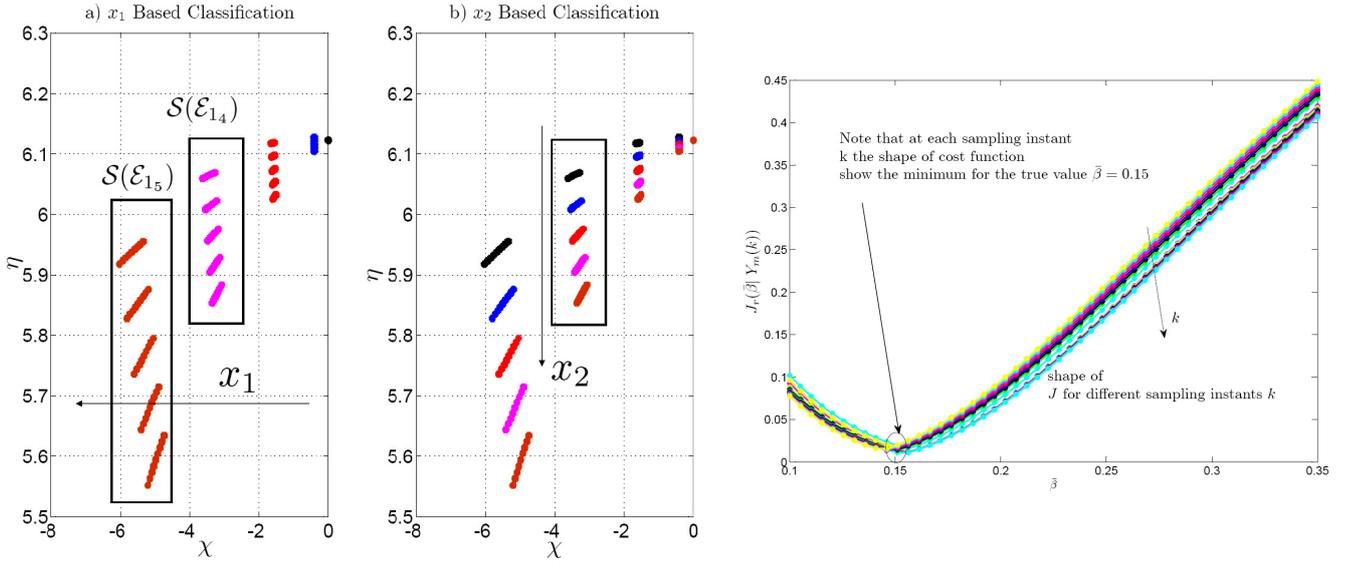$$\mathbb{Z}_d^{(1)} := \left\{ x_{1_1}, \dots, x_{1_5} \right\} \times \left\{ x_{2_1}, \dots, x_{2_5} \right\}$$

Fig. 2. Views of the 25 signatures $\mathcal{S}(z^{(1)})$ for $z^{(1)} \in \mathbb{Z}_d^{(1)}$ obtained using $N = 2$ and $\bar{\beta} = 0.15$. Note that each signatures contains $M = N_O - N = 9$ points. subplot (a) regroups all signatures sharing the same value of x_1 using the same color while subplot b) regroups them based on the value of x_2. subplot (c) The shape of the cost function $J_r(\bar{\beta} \mid Y_m(k))$ at different instants k.

This is clearly a discrete set containing 25 elements. To these 25 elements of $\mathbb{Z}_d^{(1)}$ correspond 25 signatures

$$\left\{ \mathcal{S}^N(z^{(1)}) \right\}_{z^{(1)} \in \mathbb{Z}_d^{(1)}}$$

that can be defined once a given value $N < N_O$ and $\bar{\beta}$ are chosen.

Fig. 2 shows these 25 signatures viewed differently on the two subplots a) and b). More precisely Fig 2.a) shows these 25 signatures with all those sharing the same value x_1 plotted using the same color. For instance, the five signatures in green on Fig. 2.a) are obtained for the set of values:

$$\mathcal{E}_{1_1} := \left\{ (x_{1_1} = 0, x_{2_j})^T \right\}_{j=1}^{5}$$

Similarly, Fig .2b) regroups the signatures based on the values of x_2. For instance, all the signatures plotted in green are those corresponding to the set of elements in $\mathbb{Z}_d^{(1)}$ given by:

$$\mathcal{E}_{2_5} := \left\{ (x_{1_j}, x_{2_5} = 3)^T \right\}_{j=1}^{5}$$

Visual inspection of the signatures depicted in Fig. 2 shows clearly that once the signature $\mathcal{S}(z^{(1)})$ is plotted, it is possible to identify $z^{(1)} = (x_1, x_2)^T$ using the two following steps:

1) First determine x_1 based on the signature property

$$r_1(\mathcal{S}) := \min_{i \in \{1, \dots, M\}} \chi_i$$

This can be obtained by interpolating the information on Fig. 2.a), indeed:

$$\forall e \in \mathcal{E}_{1_4}, \quad r_1(\mathcal{S}) \cong -3.5$$
$$\forall e \in \mathcal{E}_{1_3}, \quad r_1(\mathcal{S}) \cong -1.5$$
$$\forall e \in \mathcal{E}_{1_2}, \quad r_1(\mathcal{S}) \cong -0.5$$
$$\forall e \in \mathcal{E}_{1_1}, \quad r_1(\mathcal{S}) \cong 0$$

and so on. For a new value of r_1, one can easily associate the corresponding value of x_1.

2) The subplot Fig 2.b) clearly shows that there is a monotonic map defined by:

$$x_2 = X_2(\eta_{min} \mid x_1)$$

that gives x_2 knowing x_1 and the property

$$\eta_{min} = r_2(\mathcal{S}) := \min_{i \in \{1, \dots, M\}} \eta_i$$

This is because once x_1 is given [thanks to $r_1(\mathcal{S})$], once knows that the tail of the signature lies approximately on a vertical line with a height that is directly linked to the value of x_2 in a bijective way.

The above discussion completely defines the invertible map (12) using the signature defined by $N = 2$ and the two signature properties r_1 and r_2. Note that it can be checked that this procedure holds for any value of $\bar{\beta} \in [0.1, 0.35]$

Once the invertible map is obtained, the scalar dimensional problem (8) can be defined in the scalar decision variable $\bar{\beta}$. Fig.2c) shows the shape of the cost function $J_r(\bar{\beta} \mid Y_m(k))$ for different instants k when the value $\bar{\beta} = 0.15$ is used to produce the measurement vector $Y_m(k)$. This clearly shows that solving this scalar optimization problem is quite easier than solving the original 3-dimensional problem.

B. Example 2:

In order to illustrate the above ideas on another concrete example, let us consider the dynamical model of recombinant *Escherichia Coli strain* ([2], [7], [9], [6]). This model is a mass balance model describing the pure recombinant microbial batch culture of *E. Coli* strain X growing on the limiting substrate glycerol S while yielding a final intracellular product β-galactosidase protei P:

$$\dot{X} = \mu(S)X - k_d \exp(-\frac{k_p}{P})X \tag{16}$$

$$\dot{S} = -y_s\mu(S)X - k_m X \tag{17}$$

$$\dot{P} = y_p\mu(S)\frac{I}{I+k_l}X - k_d \exp(-\frac{k_p}{P})P \tag{18}$$

where μ is the growth rate that is modeled using classical Monod-type relation:

$$\mu(S) = \frac{\mu_m S}{k_s + S}$$

in which μ_m is the maximum specific growth rate for the cell growth in (h^{-1}). k_s is the half saturation constant. k_p and k_d are constants involved in the Arrhenius-type death kinetic that depends on P. k_m is a maintenance rate that describes the energy required for normal upkeep and repair. y_s, y_l are identified yield coefficients. I stands for the arabinose inducer that is assumed to be constant (no degradation).

The output measurement is the light produced by the bioluminescence that is defined by the following expression:

$$L = y_l.\mu(S)\frac{I}{I+k_l}XP \tag{19}$$

In a series of recent works ([2], [7], [9]), the parameters of the above model have been identified and the resulting model has been experimentally validated using Micro-fermentor test-bed. The resulting set of values are given on table I. Here, the framework proposed in section II is applied to this

parameter	Values	Units
μ_m	0.49	h^{-1}
k_s	0.06	g/l
k_p	0.047	g/l
k_d	0.005	g/l
k_m	0.21	h^{-1}
k_l	0.03	g/l
y_s	0.75	$g \ cell/ \ g \ glycerol$
y_p	0.32	$g \ protein/ \ \beta - \ galactosidase$
y_l	17.6	$U/\beta - \ galactosidase$

TABLE I

IDENTIFIED PARAMETERS FOR THE DYNAMIC MODEL

system using the following definitions:

- $z^{(1)} := (x_1, x_3)^T$, $n_1 = 2$, $z^{(2)} = x_2$

- $\mathbb{Z}^{(1)} := [0.01, 0.09] \times [0.05, 0.15]$, $N_O = 11$, $\tau = 0.01$

Let us define the following discrete subset of $\mathbb{Z}^{(1)}$ that may be obtained using uniform grids on the admissible intervals for x_1 and x_3, namely:

$$\mathbb{Z}_d^{(1)} := \{x_{1_1}, \ldots, x_{1_5}\} \times \{x_{3_1}, \ldots, x_{3_5}\}$$

The same road map that has been used in example 1 is conducted here, namely, the signatures associated to the 25 values of $z^{(1)}$ contained in $\mathbb{Z}_d^{(1)}$ are plotted for visual inspection.

Fig. 3 shows these signatures viewed differently in the two subplots a) and b). More precisely, Fig .3 a) [resp. (b)] show these 25 signatures with all those sharing the same value x_1 [resp. x_3] plotted using the same color.
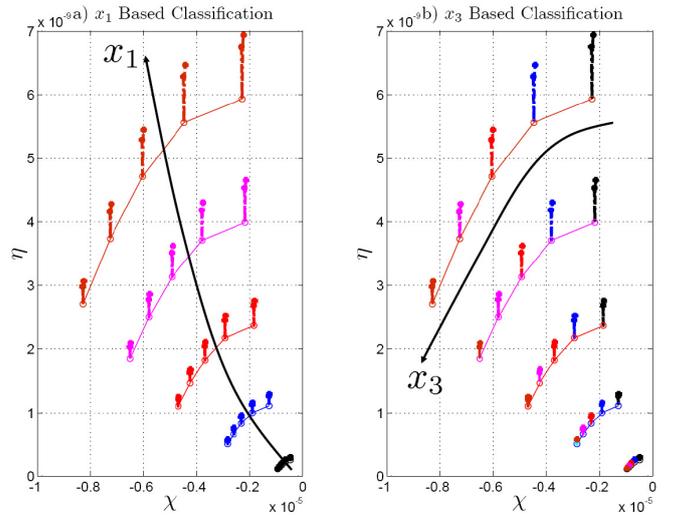

Fig. 3. Views of the 25 signatures $\mathcal{S}(z^{(1)})$ for $z^{(1)} \in \mathbb{Z}_d^{(1)}$ obtained using $N = 4$ and $x_2 = 2.5$. Note that each signatures contains $M = N_O - N = 7$ points. subplot (a) regroups all signatures sharing the same value of x_1 using the same color while subplot b) regroups them based on the value of x_3.

Visual inspection of the signatures depicted in Fig .3 shows clearly that once a signature is plotted, it is possible to identify $z^{(1)} = (x_1, x_3)^T$ using the following steps:

1) First determine x_1 based on the signature property

$$r_1(\mathcal{S}) := \text{curvilinear coordinate of the}$$
$$\text{lowest point of the signature}$$
$$\text{in the curvilinear coordinates of Fig 3.a)}$$

This can be obtained by interpolating the information on Fig .3a)

2) The subplot Fig .3b) clearly shows that there is a monotonic map defined by:

$$x_3 = X_3(\eta_{min} \mid x_1)$$

that gives x_3 knowing x_1 and the property

$$\eta_{min} = r_2(\mathcal{S}) := \min_{i \in \{1,\ldots,M\}} \eta_i$$

This is because once x_1 is given [thanks to $r_1(\mathcal{S})$], one knows that the tail of the signature lies approximately on a vertical line with horizontal position determined by the value of x_3 in a bijective way.

V. CONCLUSIONS AND FUTURE WORKS

In this paper, a novel approach has been proposed that aims at reducing the on-line computational burden associated to the moving horizon observer. This is done by off-line derivation of explicit expression of a part of the unknown vector as a function of the other part and the vector of past measurements that are available for MHO computation. The concepts have been validated through two concrete examples showing the potential efficiency of the proposed approach.

Note however that although the general framework involves the presence of controlled input in the system model, no such example have been yet studied. Future work include such investigated together with an analysis of the robustness of the proposed approach in the presence of measurement noise that may alter the quality of the invertible map. Finally, the use of the proposed scheme as a tool for the analysis of the feasibility of the inverse problem as well as general nonlinear observability may also be a promising

APPENDIX

A. Expression of the map $P_q(Y)$

Given $Y \in \mathbb{R}^{N+1}$, the following map has been suggested in [13]:

$$P_q(Y) = \Phi_0(Y) + \lambda(Y) \cdot \left[\Phi_1(Y) - \Phi_0(Y) \right] \quad (20)$$

$$\Phi_0(Y) = \frac{1}{2N} \sum_{j=1}^{N} \Psi_j(Y) \quad (21)$$

$$\Phi_1(Y) = \frac{1}{2N} \sum_{j=1}^{N} \bar{Z}_j \Psi_j(Y) \quad (22)$$

where

$$\Psi_j(Y) := \left[(1 + \bar{Z}_i) Q_{i+1} - (\bar{Z}_i - 1) Q_i \right]$$

$$\bar{Z}_i := \frac{Y_i}{\eta_n \cdot \max_{j=1}^{N} |Y_i| + 1}$$

$$Q_i := \left(\cos(\frac{2\pi(i-1)}{N}), \sin(\frac{2\pi(i-1)}{N}) \right)^T$$

$$\lambda(Y) := \frac{Y_{N+1}}{\eta_n \cdot \max_{j=1}^{N} |Y_i| + 1} - \frac{1}{N} \sum_{i=1}^{N} \bar{Z}_i$$

The vector of signature parameter q include the integer N, the normalization coefficient $\eta_n \in \{0, 1\}$ and the under-sampling integer that is not mentioned in the equation for simplicity.

REFERENCES

[1] M. Alamir, P. Bellemain, L. Boillereaux, I. Queinnec, M. Titica, N. Sheibat-Othman, C. Cadet, and G. Besançon. Clpp: A user-friendly platform for nonlinear robust observer design. In *9th International Symposium on Dynamics and Control of Process Systems (Dycops 2010)*, Leuven, Belgium, 2010.

[2] M. Alamir, N. Sheibat-Othman, and S.Othman. On the use of nonlinear receding-horizon observers in batch terpolymerization processes with partially unmodelled dynamics: Formulation and experimental validation. In *Nonlinear Control Systems*, volume 17, August 2007. (Invited session on nonlinear observers in bioreactors).

[3] M. Diehl, H. J. Ferreau, and N. Haverbeke. *Assessment and Future Directions of Nonlinear Model Predictive Control*, chapter Efficient Numerical Methods for Nonlinear MPC and Moving Horizon Estimation, pages 317–417. Springer-Verlag, 2009.

[4] G. Besançon (Ed). *Nonlinear Observers and Applications*. Lecture Notes in Control and Information Sciences. Springer-Verlag, 2007.

[5] J. P. Gauthier, H. Hammouri, and S. Othman. A simple observer for nonlinear systems – application to bio-reactors. IEEE Transactions on Automatic Control, 37, 1992.

[6] J. Valdes G. Rao H. J. Cha, C. F. Wu and W. E. Bentley. Observations of green fluorescent protein as a fusion partner in genetically engineered escherichia coli: monitoring protein expression and solubility. In *Biotech. Bioeng.*, volume 67, pages 635–646, 2000.

[7] J.Lee and F. Ramirez. Mathematical modelling of induced doreign procduction by recombinant bacteria. In *Biotech. Bioeng*, volume 29, pages 635–646, 1992.

[8] H. Michalska and D. Q. Mayne. Moving-horizon observers and observer-based control. *IEEE Transactions on Automatic Control*, 40:995–1006, 1995.

[9] M. Nardi, I. Trezzani, H. Hammouri, and P. Dhurjati. Mathematical model and observer for recombinant escherichia coli strain with bioluminescence indicator genes. In *In Proceedings of the Second International Symposium on Communications, Control and Signal Processing (ISCCSP 2006)*, 2006.

[10] Lars Imsland Rambabu Kandepu, Bjarne Foss. Applying the unscented kalman filter for nonlinear state estimation. *Journal of Process Control*, 18:753–768, August-September 2008.

[11] D. Simon. *Optimal State Estimation*. Wiley Interscience, 2006.

[12] J. E. Slotine, J. K. Hedrick, and E. A. Misawa. On sliding observers for nonlinear systems. Journal of Dynamics Sysytems, Measurements and Control, 109, 1987.

[13] B. Youssef and M. Alamir. Generic signature based tool for diagnosis and parametric estimation for multi-variable dynamical nonlinear systems. In *Proceedings of the 42th Conference on Decision and Control*, Hawa, USA, 2003.

[14] B. Youssef and M. Alamir. Diagnosis and on-line parametric estimation of automotive electronic throttle control system. In *Proceedings of the IFAC World Congress*, Praha, Czech Republic, 2005.

[15] B. Youssef, M. Alamir, and F. Ibrahim. Diagnosis and on-line parametric estimation of simulated moving bed. In *Proceedings of the 44th Conference on Decision and Control (CDC-ECC05)*, Seville, Spain, 2005.

[16] V. M. Zavala and L. T. Biegler. *Assessment and Future Directions of Nonlinear Model Predictive Control*, chapter Nonlinear Programming Sensitivity for Nonlinear State Estimation and Model Predictive Control, pages 419–432. Springer-Verlag, 2009.